# Title

Regulation of MHC-I and MHC-II by CIITA in transmissible cancers

# Authors

Chrissie E. B. Ong [a], Yuanyuan Cheng [b], Hannah V. Siddle [c, d], A. Bruce Lyons [e], Gregory M. Woods [a], Andrew S. Flies [a*]

# Affiliations

[a] Menzies Institute for Medical Research, College of Health and Medicine, University of Tasmania, Hobart, TAS, Australia

[b] School of Life and Environmental Sciences, The University of Sydney, Sydney, NSW, Australia

[c] Department of Biological Sciences, University of Southampton, Southampton, UK

[d] Institute for Life Sciences, University of Southampton, Southampton, UK

[e] Tasmanian School of Medicine, College of Health and Medicine, University of Tasmania, Hobart, TAS, Australia

# *Correspondence

**Andrew S. Flies, PhD**

Menzies Institute for Medical Research, College of Health and Medicine

University of Tasmania

Private Bag 23, Hobart TAS 7000

phone: +61 3 6226 4614; email: Andy.Flies@utas.edu.au

# Highlights

- Non-haematopoietic devil facial tumour (DFT) cells do not typically express MHC-II
- CIITA regulates components of the MHC-I and MHC-II machinery in DFT cells
- CIITA can induce MHC-I and MHC-II expression in DFT1 cells
- Serum from devils with tumour regressions binds to DFT cells that express CIITA
- MHC-II expression in transmissible cancers has implications for anti-tumour immunity

# Abstract

MHC-I and MHC-II molecules are critical components of antigen presentation and T cell immunity to pathogens and cancer. The transmissible devil facial tumour (DFT) cells that cause Tasmanian devil facial tumour disease (DFTD) exploit MHC-I pathways to overcome immunological anti-tumour and allogeneic barriers. This exploitation underpins the ongoing transmission of DFT cells across the wild Tasmanian devil population. MHC-II expression is

crucial for $CD4^+$ T cell activation and is primarily confined to haematopoietic antigen presenting cells. We discovered that the MHC-II transactivator, CIITA, can induce MHC-II expression in non-haematopoietic cells. Transcriptomic analysis of DFT cell lines revealed that CIITA can upregulate several genes of the MHC-I and MHC-II pathways, resulting in protein expression of MHC-I and MHC-II complexes. The induced expression of MHC-II in transmissible cancers signifies that CIITA can function in non-haematopoietic cancer cells and offer a novel strategy to enhance tumour recognition via MHC-II-restricted tumour antigen presentation.

## Keywords

transmissible cancer, devil facial tumor, DFTD, allograft, MHC, CIITA

## 1. Introduction

The Tasmanian devil is the largest extant carnivorous marsupial and is endemic to the island state of Tasmania. Following the emergence of devil facial tumour disease (DFTD) in 1996, the population of devils has declined precipitously, threatening the persistence of devils in the wild (Cunningham et al., 2021; Hawkins et al., 2006; Lazenby et al., 2018). DFTD is caused by two independent transmissible cancers of Schwann cell origin, referred herein as DFT1 and DFT2 (Murchison et al., 2010; Patchett et al., 2020; Pye et al., 2016b). DFT1 was discovered northeast of Tasmania in 1996 while the second tumour, DFT2, was found in 2014 in the D'Entrecasteaux channel, southeast Tasmania (Hawkins et al., 2006; Pye et al., 2016b). Both tumour types are clonal cell lines that harbour distinct genetic profiles differing from individual host devils (Pearse and Swift, 2006; Pye et al., 2016b). DFT cells are transmitted as a malignant allograft amongst devils through social interactions.

Genetic differences between host and tumour, particularly at the major histocompatibility complex (MHC) loci (Siddle et al., 2007), should induce immune-mediated allograft rejection. However, the 25 years of ongoing DFT1 transmission suggests that DFT1 cells have evolved to evade immune defences. The lack of anti-DFT immune responses has predominantly focused on the loss of MHC-I from the surface of DFT1 cells. This occurs via epigenetic downregulation of several components of the MHC-I antigen processing pathway (Siddle et al., 2013) and a hemizygous deletion of beta-2 microglobulin (*B2M*), which is necessary for stabilising MHC-I complexes on the cell surface (Stammnitz et al., 2018). Natural and immunotherapy-induced tumour regressions have been observed in devils, along with antibody responses to DFT1 cells, albeit primarily in the context of MHC-I (Ong et al., 2021; Pye et al.,

2016a; Tovar et al., 2017). Conversely, the emerging DFT2 tumours do express MHC-I (Caldwell et al., 2018), suggesting that other immune evasion mechanisms are important.

Given the role of MHC-I in antigen display and anti-DFT humoral response, the manipulation of MHC-I expression on DFT cells is an attractive target to improve host responses towards DFT cells and mitigate the effects of disease in the wild devil population. An upregulation of MHC-I on DFT cells should enhance MHC-I-restricted tumour-specific cytotoxic $CD8^+$ T cell response. However, this approach alone proved to be insufficient for eliciting protective immunity, as exemplified in immunisation trials of naïve devils against DFT1 (Pye et al., in press; Tovar et al., 2017). Although $CD8^+$ T cells are recognised as the major effector cells in tumour elimination, $CD4^+$ T cell help is shown to be critical in facilitating an effective anti-tumour immune response (reviewed in (Ostrand-Rosenberg, 2005; Tay et al., 2020)). $CD4^+$ helper T cells play a multifaceted role of orchestrating the adaptive and humoral immune response. From cytokine production to expression of co-stimulatory molecules, $CD4^+$ helper T cells initiate, augment, and sustain the effector function of not only $CD8^+$ T cells and B cells but also innate cells (Bennett et al., 1998; Hung et al., 1998; Janssen et al., 2003; Kumamoto et al., 2011). Moreover, $CD4^+$ T cells are capable of initiating allograft rejection independently of $CD8^+$ T cells (Dalloul et al., 1996; Krieger et al., 1996; Pietra et al., 2000).

The activation of $CD4^+$ T cells involves recognition of antigens presented on MHC-II complexes. In contrast to MHC-I, constitutive expression of MHC-II is restricted to thymic epithelial cells, activated human T cells, and professional antigen presenting cells (APCs) such as B cells, dendritic cells, and macrophages. However, *de novo* MHC-II expression can be induced in non-haematopoietic cells including tumour cells by the inflammatory cytokine interferon gamma (IFNG) (Carrel et al., 1985; Hirsch et al., 1983; Propper et al., 2003). Both constitutive and IFNG-induced expression of MHC-II genes are mediated by the Class II transactivator (CIITA), making it the master regulator of MHC-II expression (Steimle et al., 1994, 1993). Additionally, CIITA is capable of modulating the expression of MHC-I, particularly in cell lines with low to no MHC-I expression (Gobin et al., 1997; Martin et al., 1997).

The presence of MHC-II molecules in DFT cells has not been described, although CIITA and some MHC-II transcripts can be upregulated *in vitro* in DFT1 cells with IFNG treatment (Siddle et al., 2013). We have previously genetically modified DFT1 and DFT2 cells that overexpress the MHC-I transactivator NLRC5 to induce stable expression of MHC-I on the

cell surface (Ong et al., 2021). The lack of MHC-II expression in DFT cells provided an opportunity to conduct similar investigations into the role of CIITA in MHC-II regulation in marsupials and transmissible cancers. Transcriptomic and protein-based analyses showed that CIITA upregulates the expression of genes associated with MHC-I and MHC-II antigen processing and presentation in DFT cells. The ability to modulate antigen presentation in transmissible cancer cells in the context of MHC uncovers additional targets for anti-tumour immune response and the potential for recruitment of $CD4^+$ T cell help.

# 2. Materials and methods

## 2.1 Cells and cell culture conditions

Cell lines that were used in this study include DFT1 cell line C5065 strain 3 (Pearse et al., 2012) (RRID:CVCL_LB79), and DFT2 cell lines: RV (RRID:CVCL_LB80) and JV (RRID:CVCL_A1TN) (Pye et al., 2016b) (**Table 1**). DFT1 C5065 was provided by A-M Pearse and K. Swift of the Department of Primary Industries, Parks, Water and Environment (DPIPWE) (Hobart, TAS, Australia) and was previously established from DFT1 biopsies obtained under the approval of the Animal Ethics Committee of the Tasmanian Parks and Wildlife Service (permit numbers A0017090 and A0017550) (Pearse et al., 2012). DFT2 cell lines RV and JV were established from single cell suspensions obtained from tumour biopsies (Pye et al., 2016b). Cells were cultured at 35 °C with 5% $CO_2$ in Gibco™ RPMI 1640 medium with L-glutamine (Thermo Fisher Scientific, Waltham, MA, USA) supplemented with 10% heat-inactivated fetal bovine serum (Bovogen Biologicals, Melbourne, VIC, Australia), 1% (v/v) Gibco™ Antibiotic-Antimycotic (100X) (Thermo Fisher Scientific), 10 mM Gibco™ HEPES (Thermo Fisher Scientific) and 50 μM 2-mercaptoethanol (Sigma-Aldrich, St. Louis, MO, USA) (complete RPMI medium).

## 2.2 Plasmid construction

The coding sequence for full length devil *CIITA* (XM_023497584.2) was isolated from cDNA of devil peripheral blood mononuclear cells (PBMCs) by PCR using Q5® Hotstart High-Fidelity 2X Master Mix (New England Biolabs (NEB), Ipswich, MA, USA) (see **Supplementary Table 1** for list of primers and reaction conditions). Sleeping Beauty (SB) transposon plasmid pSBbi-BH (Kowarz et al., 2015) (a gift from Eric Kowarz; Addgene # 60515, Cambridge, MA, USA) was digested at SfiI sites (NEB) with the addition of Antarctic Phosphatase (NEB) to prevent re-ligation. Devil *CIITA* was then cloned into SfiI-digested pSBbi-BH using NEBuilder® HiFi DNA Assembly Cloning Kit (NEB). The assembled plasmid

pCO2 was transformed into NEB® 5-alpha competent *Escherichia coli* (High Efficiency) (NEB) according to manufacturer's instructions (see **Supplementary Figure 1** for plasmid maps). Positive clones were identified by colony PCR and the plasmids were isolated using NucleoSpin® Plasmid EasyPure kit (Macherey-Nagel, Düren, Germany). The DNA sequence of the cloned devil *CIITA* transcript was verified by Sanger sequencing using Big Dye™ Terminator v3.1 Cycle Sequencing Kit (Applied Biosystems (ABI), Foster City, CA, USA) and Agencourt® CleanSEQ® (Beckman Coulter, Brea, CA, USA) per manufacturer's instructions. The sequences were analyzed on 3500xL Genetic Analyzer (ABI) (see **Supplementary Table 2** for list of sequencing primers). For detailed step-by-step protocols for plasmid design and construction, reagent recipes, and generation of stable cell lines, see Bio-protocol # e3986 (Flies et al., 2020).

## 2.3 Transfection and generation of stable cell lines

DFT1 and DFT2 cell line C5065 and JV, respectively, were transfected with plasmid pCO2 to generate stable cell lines that overexpress CIITA. DNA transfections were performed using polyethylenimine (PEI) (1 mg/mL, linear, 25 kDa; Polysciences, Warrington, FL, USA) at a 3:1 ratio of PEI to DNA (w/w) as previously described (Ong et al., 2021). Briefly, DFT cells were co-transfected with pCO2 and SB transposase vector pCMV(CAT)T7-SB100 (Mátés et al., 2009) (a gift from Zsuzsanna Izsvak; Addgene plasmid # 34879) at a ratio of 3:1 in µg, respectively. One µg of total plasmid DNA was used per mL of culture volume. The cells were incubated with the transfection solution overnight at 35 °C with 5% $CO_2$. The media was removed and replaced with fresh complete RPMI medium. 48 h post-transfection, the cells were observed for expression of reporter gene mTagBFP. Positively-transfected cells were selected with 1 mg/mL hygromycin B (Sigma-Aldrich) for seven days before being maintained in 200 µg/mL hygromycin B in complete RPMI medium. The two tumour cell lines were also transfected with empty vector pSBbi-BH as controls.

## 2.4 RNA sequencing and analysis

RNA libraries were prepared, sequenced and processed as previously described (Ong et al., 2021; Patchett et al., 2020, 2018). **Table 1** shows the source of RNA samples used in this study. Briefly, RNA extraction (two replicates per cell line) was performed using the Nucleospin® RNA Plus Kit (Macherey-Nagel) following the manufacturer's instructions. mRNA libraries were prepared and sequenced at the Ramaciotti Centre for Genomics (Sydney, NSW, Australia). All RNA samples had RNA Integrity Number (RIN) scores of 10.0. Libraries were

prepared using TruSeq Stranded mRNA Library Prep (Illumina Inc., San Diego, CA, USA) and single-end, 100-base pair sequencing were performed on an Illumina NovaSeq 6000 platform (Illumina). The quality of the sequencing reads was assessed using FastQC version 0.11.9 (Andrews, 2010). Raw FASTQ files for DFT1.CIITA and DFT2.CIITA have been deposited to the European Nucleotide Archive (ENA) and are available at BioProject # PRJEB45867.

Subread version 2.0.0 (Liao et al., 2013) was used to align sequencing reads to the Tasmanian devil reference genome (GCA_902635505.1 mSarHar1.11) and the number of reads mapped to a gene was counted using featureCounts (Liao et al., 2014). The analysis of differentially expressed genes was performed using the statistical software R studio (RStudio Team, 2020) on R version 4.0.0 (R Core Team, 2020). Genes with less than 100 aligned reads across all samples were excluded from the analysis and raw library sizes were scaled using *calcNormFactors* in edgeR (Anders and Huber, 2010; Robinson et al., 2009; Robinson and Oshlack, 2010). To account for varying sequencing depths between lanes, read counts were normalised by upper quartile normalisation using *betweenLaneNormalization* in EDASeq (Bullard et al., 2010; Risso et al., 2011). Gene length-related biases were normalised by scaling read counts to transcripts per kilobase million (TPM). Differential expression analysis was carried out using the *voom* (Law et al., 2014) function in *limma* (Ritchie et al., 2015) with linear modelling and empirical Bayes moderation (Phipson et al., 2016). To isolate differentially expressed genes, gene expression of CIITA- or NLRC5-expressing cell lines (DFT.CIITA, DFT.NLRC5) was compared against vector-only control (DFT.BFP) while IFNG-treated cells (DFT.WT + IFNG) was compared against untreated cells (DFT.WT), according to their respective tumour origin. Genes were defined as significantly differentially expressed by applying false discovery rate (FDR) $< 0.05$, and $\log_2$ fold change (FC) $\geq 2.0$ (upregulated) or $\leq -2.0$ (downregulated) thresholds (see **Supplementary Table 3** for list of differentially expressed genes).

Venn diagrams of differentially expressed genes were developed using Venny version 2.1 (Oliveros, 2015). Heatmaps were created from $\log_2$(TPM) values using the ComplexHeatmap (Gu et al., 2016) package in R studio. For functional enrichment analysis, over-representation of gene ontology (GO) biological processes in the list of differentially expressed genes was performed using Database for Annotation, Visualization and Integrated Discovery (DAVID) functional annotation tool (Huang et al., 2009a; b). The Tasmanian devil *Sarcophilus harrisii* was applied as the species for gene lists and background. Significant GO terms

(GOTERM_BP_ALL) were selected by applying the following thresholds: p-value < 0.05 and FDR < 0.05. GO terms were sorted in descending order of fold enrichment values.

To simplify the identification of devil MHC allotypes and maintain consistency in nomenclature to previous works, MHC transcripts in this manuscript were renamed according to Cheng et al., based on sequence similarity (Cheng et al., 2012) (see **Supplementary Table 4** for corresponding NCBI gene symbols). MHC transcripts *LOC100918485* and *LOC100918744*, which have not been previously characterised, are predicted to encode beta chains of the MHC-II DA gene based on gene homology. These transcripts were renamed as *SAHA-DAB_X1* and *SAHA-DAB_X2*, respectively. Similarly, genes without an official gene symbol (LOC prefixes) were given aliases based on the gene description on NCBI.

## 2.5 Flow cytometric analysis of B2M and MHC-II expression

Cultured cells were harvested using TrypLE™ Express Enzyme (1X) (Thermo Fisher Scientific) and counted using a haemocytometer. $1\times10^5$ cells per well were aliquoted into round-bottom 96-well plates and washed with 1X PBS (Thermo Fisher Scientific). Washing steps include centrifugation at 500*g* for 3 min at 4 °C to pellet cells before removal of supernatant. Cells were first stained with Invitrogen™ LIVE/DEAD™ Fixable Near-IR Dead Cell Stain kit (Thermo Fisher Scientific) diluted according to manufacturer's instructions for 30 min on ice, protected from light. After staining, cells were washed twice with 1X PBS. For MHC-II expression, a monoclonal mouse antibody against the intracellular tail of human HLA-DR α chain was used (Clone TAL.1B5, # M0746, Agilent, Santa Clara, CA, USA). Detection of MHC-I on the surface of cells was performed using a monoclonal mouse antibody against devil beta-2-microglobulin (B2M) in supernatant (Clone 13-34-45; a gift from Hannah Siddle (Siddle et al., 2013)). Cells for intracellular staining of HLA-DR were first fixed and permeabilised using BD Cytofix/Cytoperm™ Plus Fixation/Permeabilization Kit (BD Biosciences, North Ryde, NSW, Australia). All intracellular antibody staining, and washes were carried out in 1X BD Perm/Wash™ Buffer (BD Biosciences) while FACS buffer (PBS with 0.5% BSA, 0.02% sodium azide) was used for surface antibody staining. All cells were incubated with 1% normal goat serum (Thermo Fisher Scientific) for blocking, 10 min on ice. After that, cells were washed and incubated with either anti-human HLA-DRα (0.48 μg/mL) or anti-devil B2M antibody (1:250 v/v dilution) for 30 min on ice. Cells were washed once and stained with goat anti-mouse IgG-Alexa Fluor 488 (2 μg/mL, # A11029, Thermo Fisher Scientific) for 30 min on ice, in the dark. Two final washes were given to remove excess secondary antibody. Fixed cells were resuspended in FACS buffer while the rest were

resuspended in FACS fix solution (0.02% sodium azide, 1.0% glucose, 0.4% formaldehyde). Analysis was carried out using Cytek™ Aurora (Cytek Biosciences, Fremont, CA, USA). As a positive control for MHC-I expression, DFT cells were treated with 10 ng/mL devil recombinant IFNG (Flies et al., 2016) for 24 h.

## 2.6 Protein extraction and western blot

Cells were harvested and centrifuged at 500*g* for 5 min at room temperature. The pellet was washed twice with cold 1X PBS and weighed. Total cell protein was extracted by adding 1 mL RIPA Lysis and Extraction Buffer (Thermo Fisher Scientific), 10 µL Halt™ Protease Inhibitor Cocktail (Thermo Fisher Scientific) and 10 µL Halt™ Phosphatase Inhibitor Cocktail (Thermo Fisher Scientific) per 40 mg of wet cell pellet. The suspension was sonicated for 30 seconds with 50% pulse and then mixed gently for 15 min on ice. The mixture was centrifuged at 14000*g* for 15 min to pellet the cell debris. The supernatant was transferred to a new tube and total protein was quantified using EZQ® Protein Quantitation kit (Invitrogen) according to manufacturer's instructions. Two replicates per cell line were prepared for protein extraction.

20 µg of protein per sample was used for target protein detection by western blot. Protein samples were subjected to SDS-PAGE using Bolt™ 4-12%, Bis-Tris, 1.0 mm Mini Protein Gel (Thermo Fisher Scientific). Briefly, protein samples were treated with 1X Bolt™ LDS Sample Buffer (Thermo Fisher Scientific) and 1X Bolt™ Reducing Agent (Thermo Fisher Scientific) at 70 °C for 10 min. Samples were loaded onto the gel and run with 1X Bolt™ MES SDS Running Buffer (Thermo Fisher Scientific) in the Mini Gel Tank (Thermo Fisher Scientific) at 100 V for 5 min followed by 200 V for 15 min. SeeBlue™ Plus2 Pre-stained Protein Standard (Thermo Fisher Scientific) was used as a molecular weight marker. Proteins were transferred to a nitrocellulose membrane using iBlot™ Transfer Stack, nitrocellulose, mini (Thermo Fisher Scientific) and iBlot™ Gel Transfer Device (Thermo Fisher Scientific) using the following settings: 20 V for 7.5 min.

For immunodetection, the membrane was blocked with TBSTM (Tris-buffered saline (TBS): 50 mM Tris-HCl, 150 mM NaCl, pH 7.6), 0.05% Tween 20, and 5% skim milk) for 1 hour at room temperature and rinsed twice with TBST (TBS, 0.05% Tween 20). Then, the membrane was incubated with: (i) rabbit polyclonal anti-beta actin antibody (# ab8227, Abcam, Cambridge, UK) diluted in TBSTM (400 ng/mL), (ii) mouse monoclonal anti-devil SAHA-UA/UB/UC in supernatant (Clone 15-25-18; a gift from Hannah Siddle (Caldwell et al., 2018)), or (iii) mouse monoclonal anti-devil SAHA-UK in supernatant (Clone 15-29-1; a gift from

Hannah Siddle (Caldwell et al., 2018)) overnight at 4 °C. The membranes were washed four times with TBST for a duration of 5 min each wash. After that, the membranes were incubated with either HRP-conjugated goat anti-mouse (250 ng/mL; # P0447, Agilent) or HRP-conjugated goat anti-rabbit immunoglobulin (62.5 ng/mL; # P0448, Agilent) diluted in TBSTM for 1 hour at room temperature. The membranes were given final washes as described above. All incubation and washing steps were performed under agitation. Target protein expression was detected using Immobilon™ Western Chemiluminescent HRP Substrate (Merck Millipore, Burlington, MA, USA) according to manufacturer's protocol. Protein bands were visualised using Amersham™ Imager 600 (GE Healthcare Life Sciences, Malborough, MA, USA).

## 2.7 Flow cytometric analysis of serum antibody binding

Serum samples from four devils (My, TD4, TD5, and TD6), collected before (pre-immune) and after DFT1 clinical manifestations (immune), were used to assess antibody responses towards CIITA-expressing DFT cell lines (**Supplementary Table 5**). The serum samples were identified as immune from the presence of anti-DFT1 antibodies, which were found to be predominantly against MHC-I on DFT1 cells (Ong et al., 2021). 'My' was a devil that was immunised, challenged with DFT1 cells, and subsequently treated with an experimental immunotherapy that induced tumour regression (Tovar et al., 2017). TD4, TD5, and TD6 were naturally DFT1-infected wild devils with either spontaneous tumour regressions (TD4); MHC-II$^{+}$ and CD3$^{+}$ tumour-infiltrating lymphocytes in the tumour (TD5); or B2M$^{+}$ DFT1 cells in fine needle aspirations of a tumour (TD6) (Pye et al., 2016a). A devil with no clinical signs of DFTD during serum collection (TD7) was included as a negative control for antibody binding towards the DFT cell lines.

Cells were harvested and aliquoted into round-bottom 96-well plates as indicated above. After washing with PBS, cells were stained with LIVE/DEAD™ Fixable Near-IR Dead Cell Stain for 30 min on ice and washed twice with PBS. For blocking, cells were incubated with 1% normal goat serum for 10 min and washed once with FACS buffer. Serum samples were thawed on ice and diluted with FACS buffer (1:50 v/v). 50 µL of serum was added to cells for 1 h and then washed. After that, cells were stained with 10 µg/mL monoclonal mouse anti-devil IgG antibody (A4-D1-2-1, provided by WEHI) (Howson et al., 2014) diluted in FACS buffer for 30 min. The cells were washed and stained with 2 µg/mL goat anti-mouse IgG-Alexa Fluor 647 (# A21235, Thermo Fisher Scientific) in FACS buffer for 30 min. After washing, cells were fixed in FACS fix solution and analysed on Cytek™ Aurora. All washing steps include

two washes with FACS buffer unless indicated otherwise and all staining steps were carried out on ice, protected from light.

# 3. Results

## 3.1 CIITA plays a dominant role in antigen presentation

To delineate the role of CIITA in DFT cells, differentially expressed genes following stable expression of CIITA were analysed by gene ontology (GO) functional enrichment analysis. Differential expression analysis revealed 888 genes, excluding CIITA, that were modulated ($|\log_2 FC| \geq 2$, FDR < 0.05) in DFT1.CIITA compared to vector-only cell line DFT1.BFP (**Fig. 1**, **Supplementary Table 3**). In DFT2.CIITA, there were 56 genes that were differentially expressed relative to DFT2.BFP. Ten genes were commonly up- or down-regulated by CIITA in DFT1 and DFT2 cells. Most of these genes were of the MHC-II antigen processing and presentation pathway. *SAHA-DAA*, *SAHA-DAB2* and *SAHA-DAB3* are devil classical MHC-II genes while *SAHA-DMA* and *SAHA-DMB* encode non-classical MHC-II. Others include *CD74* and gamma-interferon-inducible lysosomal thiol reductase (*IFI30*), which encode the invariant chain, an MHC-II chaperone, and an enzyme for lysosomal degradation of proteins, respectively. Except for *IFI30*, these genes were among the most highly upregulated genes in the transcriptome of DFT1.CIITA (**Table 2**) and DFT2.CIITA (**Table 3**).

In DFT1.CIITA, several MHC-I heavy chain and accessory genes were strongly induced, depicting a role of CIITA in MHC-I antigen presentation (**Table 2**). These include: (i) MHC-I heavy alpha chain genes *SAHA-UA*, *SAHA-UB*, and *SAHA-UC*; and (ii) *B2M*, which associates with MHC-I alpha chains to form the trimeric structure of MHC-I molecules; (iii) transporter associated with antigen processing 1 (*TAP1*) for peptide transport into the endoplasmic reticulum; and (iv) proteasomal subunits *PSMB8* and *PSMB9*.

Next, all significantly up- or down-regulated genes were analysed for enriched GO biological processes using DAVID bioinformatics resource. Thresholds $p$ value < 0.05 and FDR < 0.05 were applied to filter out insignificant over-represented GO terms. The most significantly enriched GO biological process in the list of upregulated genes in DFT1.CIITA and DFT2.CIITA was *antigen processing and presentation* (GO:0019882) followed by *immune response* (GO:0006955) (**Table 4**). Both processes were identified in genes of the MHC-I and MHC-II machinery (**Supplementary Tables 6** and **7**). C*ell adhesion* (GO:0007155) and *cell communication* (GO:0007154) were enriched in genes downregulated in DFT1.CIITA; there

were no GO biological processes that were associated with downregulated genes in DFT2.CIITA.

## 3.2 Regulation of MHC-I and MHC-II pathway by CIITA

To further characterise the regulation of MHC-I and MHC-II by CIITA and how it differs from IFNG or NLRC5 stimulation, a heatmap was used to display the relative expression of MHC-I and MHC-II genes, and key accessory proteins between the different treatments. The transcriptome of IFNG-treated DFT2 cells was previously carried out on DFT2 cell line RV (DFT2.WT$^{RV}$) (Patchett et al., 2020) while subsequent experiments on DFT2 cells were performed using DFT2 cell line JV (DFT2.WT). Schwann cell differentiation marker SRY-box 10 (*SOX10*) and neuroepithelial marker nestin (*NES*) were used as internal gene controls, and myelin protein periaxin (*PRX*) was used to discriminate DFT1 cells from DFT2.

As described above, CIITA induced the transcription of *B2M;* MHC-I heavy chains *SAHA-UA*, *-UB*, *-UC*; *PSBM8; PSMB9;* and *TAP1* in DFT1 cells. There was also an upregulation of non-classical MHC-I *SAHA-UK*, and downregulation of *NLRC5* and proteasomal subunit *PSBM10* in DFT1.CIITA cells (**Fig. 2**). Excluding *NLRC5*, genes that were modulated in DFT1.CIITA were synonymously up- or down-regulated in DFT1.NLRC5, suggesting similar roles of CIITA to NLRC5 in DFT1 cells. However, induction of the MHC-I pathway by CIITA was not as strong as NLRC5 despite having similarly high levels of expression in the respective cell lines (**Fig. 2**, **Supplementary Table 3**). IFNG exhibited a wider range in regulation of genes from the MHC-I pathway compared to NLRC5 and CIITA. Peptide transporter *TAP2* and MHC-I chaperone TAP binding protein (*TAPBP*) were exclusively upregulated by IFNG in DFT1 and DFT2 cells. Meanwhile, the expression of CIITA in DFT2 cells did not appear to significantly influence any of the MHC-I machinery.

High levels of CIITA transcripts in DFT1.CIITA was correlated with strong induction of all the MHC-II genes, with *SAHA-DAB_X1* and *SAHA-DAB_X2* being the weakest. This was not observed in the other cell lines nor in DFT2.CIITA. CIITA was expressed to a lesser extent in DFT2.CIITA relative to DFT1.CIITA, and all MHC-II genes but *SAHA-DAB_X1* and *SAHA-DAB_X2* were upregulated. The expression of *CIITA*, MHC-II genes and *CD74* was relatively low in DFT1.WT and DFT2.WT cells except for *SAHA-DAB2* and *SAHA-DAB3* in DFT1.WT. There was a moderate increase in CIITA expression after IFNG treatment in DFT1 cells, but it was insufficient to initiate transcription of MHC-II genes or *CD74*. In IFNG-treated DFT2 cells where CIITA was induced to a higher degree, there was only partial activation of the MHC-II

gene set (*SAHA-DAA*, *SAHA-DMA*, *SAHA-DMB*), and an upregulation of *CD74*. Interestingly, MHC-II protease cathepsin *CTSS* was only induced with IFNG treatment in DFT1 and DFT2 cells.

## 3.3 MHC-I and MHC-II molecules are upregulated by CIITA in DFT cells

MHC-II (HLA-DRA) protein expression was absent in wild type (WT) DFT1 and DFT2 cells and in vector-only transfected cells (BFP) but was significantly upregulated in CIITA-expressing DFT1 cells (**Fig. 3A**). In DFT2 cells, the overexpression of CIITA did not alter median MHC-II expression, or more specifically MHC-II gene loci HLA-DRA. Neither IFNG treatment nor NLRC5 overexpression induced MHC-II protein expression in DFT1 and DFT2 cells.

CIITA was capable of restoring surface expression of B2M in DFT1 cells, albeit to a lesser degree than NLRC5 and IFNG stimulation, consistent with the transcriptomic results (**Fig. 3A**, **Fig. 2**). Meanwhile the basal expression of B2M in DFT2 cells was enhanced slightly by CIITA.

In agreement with an increase in surface B2M expression on DFT1.CIITA by flow cytometry, an upregulation of MHC-I heavy chains was detected by western blot compared to wild type (DFT1.WT) and vector-only cells (DFT1.BFP) (**Fig. 3B**). IFNG-treated and NLRC5-overexpressing DFT1 and DFT2 cells also expressed elevated levels of MHC-I heavy chains. Although flow cytometry detected an increase in B2M expression on DFT2.CIITA, the expression of MHC-I heavy chains by western blot was similar to DFT2.WT and DFT2.BFP.

## 3.4 Analysis of anti-DFT serum antibody response against CIITA-induced antigens

We have previously shown that MHC-I on DFT1 cells is the predominant antibody target in devils with natural and induced anti-DFT immune response including tumour regressions (Ong et al., 2021). Here we tested if expression of CIITA in DFT cells could also upregulate antibody targets on DFT cells. Four devils (My, TD4, TD5, TD6) that developed DFT1 tumours and subsequent serum antibodies (immune) that bound MHC-I were selected for screening against CIITA-expressing DFT1 and DFT2 cells. Serum from each devil prior to DFT1 infection or observable DFT1 tumours (pre-immune) was included to assess the change in antibody levels after DFT1 infection.

Relative to MHC-I negative DFT1.WT and DFT1.BFP, serum antibodies from all four devils post-DFT1 development generally showed higher binding to DFT1 cells overexpressing

NLRC5 (**Fig. 4**). Antibody levels against CIITA-expressing DFT1 cells were higher than DFT1.WT and DFT1.BFP in immune sera from My, a captive devil with an immunotherapy-induced DFT1 regression, and TD4, a wild devil with a natural DFT1 regression. Binding of serum antibodies to DFT1.CIITA cells was relatively lower than DFT1.NLRC5. There was no increase in antibody binding towards DFT1.CIITA compared to DFT1.WT and DFT1.BFP from immune sera of devils TD5 and TD6.

Serum from DFT1-infected devils reacted with DFT2 cells but only following NLRC5 overexpression. Serum from My, TD4, TD5 and TD6 all had strong antibody binding to DFT2.NLRC5 which was not observed in the other DFT2 cell lines. This suggests that NLRC5 upregulates similar antigenic target(s) in DFT1 and DFT2 cells.

# 4. Discussion

Clonally transmissible cancers in nature are rare, and yet the Tasmanian devils are affected by two of the only three known naturally occurring transmissible cancers in vertebrates. In a cancer where allogeneity exists between individual host tissues and tumour, allogeneic MHC molecules on tumour cells are important targets for anti-tumour immunity. MHC-I expression on DFT1 cells has been exploited for vaccine development and immunotherapy to enhance anti-DFT immunity via $CD8^+$ T cell responses (Tovar et al., 2017). In this study, we showed that the class II transactivator CIITA can modulate MHC-I and MHC-II antigen processing and presentation pathways in DFT cells. Surprisingly, the overexpression of CIITA resulted in upregulation of MHC-I and MHC-II molecules in DFT1 cells but not DFT2 cells.

MHC-II expression is normally confined to a subset of haematopoietic antigen-presenting cells, and DFT1 and DFT2 cells do not typically express MHC-II genes and proteins. We demonstrated the induction of MHC-II expression in non-haematopoietic DFT1 cells through CIITA-induced upregulation of classical and non-classical MHC-II genes, and the invariant chain *CD74*. The lack of detectable MHC-II proteins in CIITA-expressing DFT2 cells could be due to CIITA regulation of MHC-II expression in a quantitative manner. mRNA levels of *CIITA* were noticeably higher in DFT1.CIITA cells compared to DFT2.CIITA, and this corresponded to mRNA levels of MHC-II genes. In a study conducted on various tissues and cell lines, CIITA expression was shown to be the rate-determining factor for MHC-II expression at both mRNA and protein levels (Otten et al., 1998). The amount of MHC-II transcripts induced in CIITA-expressing DFT2 cells could be insufficient for MHC-II complex formation, especially if MHC-II genes are also regulated post-transcriptionally (Caplen et al.,

1992). No mutations have been identified in genes of the MHC-II machinery but a heterozygous non-synonymous mutation (D59N) in MHC-I and MHC-II transcription factor *RFX5* is present in DFT2 RV cell line (Stammnitz et al., 2018). This mutation was not identified in *RFX5* transcripts in DFT2.CIITA of JV cell line; however, the function of this RFX5 mutation in DFT cells and more broadly MHC-I and MHC-II expression remains to be explored.

Differential expression of MHC-II allotypes upon CIITA induction, as observed with *SAHA-DAB_X1* and *SAHA-DAB_X2* that were consistently expressed at lower levels compared to other MHC-II genes, suggests additional regulatory mechanism(s) that control the expression of MHC-II genes beyond that of CIITA. Variations in expression levels of MHC-I and MHC-II genes have been associated with sequence polymorphism in the promoter or 3' untranslated region (UTR) of MHC genes, which modulates transcription either epigenetically or non-epigenetically; as well as post-transcriptional regulation (Andersen et al., 1991; Kulkarni et al., 2011; Leen and Gorski, 1996). The varying degrees of inducibility and expression of devil MHC-II allotypes could correlate to tissue-specific expression, with functions that differ from classical MHC-II genes.

Consistent with findings from pioneering studies on CIITA function (Gobin et al., 1997; Martin et al., 1997), CIITA in DFT cells also exhibited transcriptional activity on the MHC-I pathway, particularly in cells lacking MHC-I expression. The ability of CIITA to regulate MHC-I expression is attributed to similarities in the regulatory elements at the proximal promoters of MHC-I and MHC-II genes, and interaction with the same multiprotein complex as NLRC5 (Gobin et al., 2001, 1997; Martin et al., 1997; Masternak et al., 2000; Meissner et al., 2012). In MHC-I positive DFT2 cells, overexpression of CIITA resulted in minimal upregulation of MHC-I compared with NLRC5 or IFNG stimulation. The limited CIITA influence on MHC-I expression is commonly observed in cells with high constitutive levels of MHC-I (Gobin et al., 1997; Martin et al., 1997). This illustrates the role of NLRC5 as the primary transactivator for MHC-I expression and a secondary role for CIITA.

Unlike MHC-I, which is expressed in all nucleated cells, MHC-II expression is tightly regulated in a cell type-, differentiation-, and stimulus-specific manner. However, evidence for inducibility of MHC-II transcription and proteins in DFT cells suggests that MHC-II-restricted tumour antigen presentation could occur in the physiological setting under inflammatory conditions that upregulate CIITA. This could provide additional targets for allogeneic antibody

responses, as our results show that CIITA upregulation increases binding of serum antibodies collected from devils that had both natural and immunotherapy-induced DFT1 regressions.

The capacity to express MHC-II molecules with CIITA expression could stem from the Schwann cell origins of DFT1 and DFT2 cells (Murchison et al., 2010; Patchett et al., 2020). Schwann cells express MHC-II molecules upon traumatic and inflammatory injury, playing a role in antigen presentation to $CD4^+$ T cells to modulate local immune responses (Meyer zu Hörste et al., 2010a; b). Similarly, CIITA-expressing DFT cells have the potential to present MHC-II-restricted tumour antigens to $CD4^+$ T cells and potentiate anti-DFT immune responses. Several studies in murine models have demonstrated immune-mediated tumour rejection and/or tumour growth retardation using MHC-II-expressing tumour cell lines, either through CIITA or MHC-II gene transfer (Ekkirala et al., 2014; Frangione et al., 2010; Meazza et al., 2003; Mortara et al., 2009; Ostrand-Rosenberg et al., 1990, 1989). These primary responses were also protective against subsequent challenge with parental MHC-II negative tumours. The expression of MHC-II on CIITA-expressing DFT cells can offer insight into the importance of $CD4^+$ T cells and the interplay with other immune cells for anti-tumour immunity and allograft rejection.

# 5. Conclusion

The role of CIITA as the master regulator of MHC-II expression was reaffirmed in a non-model immunology research species. We have delineated the regulation of MHC-I and MHC-II pathways by CIITA in marsupials and transmissible cancers. The ability to induce MHC-II expression in transmissible tumour cells creates an avenue for vaccine and immunotherapeutic strategies to enhance anti-tumour immunity through $CD4^+$ T cell help and inform of the importance of MHC-II in anti-tumour and allogeneic immune responses. The relatively simple process we developed for making cell lines that constitutively express NLRC5 and CIITA can be readily adapted for many other species and potentially be used in conjunction with CD80/CD86 to provide antigen stimulation in *in vitro* assays. This is critical for 99% of species that lack reagents, such as agonistic anti-CD3 and anti-CD28 antibodies, for inducing T cell activation *in vitro*.

# Declaration of competing interest

The authors declare that the research was conducted in the absence of any commercial or financial relationships that could be construed as a potential conflict of interest.

## Funding

This work was supported by the Australian Research Council (ARC) DECRA grant # DE180100484 and ARC Discovery grant # DP180100520, University of Tasmania Foundation Dr. Eric Guiler Tasmanian Devil Research Grant through funds raised by the Save the Tasmanian Devil Appeal (2013, 2015, 2017).


## Authors' contributions

ABL, ASF, CEBO and GMW designed the study. ASF and CEBO developed the technology. CEBO performed the experiments and bioinformatic analyses. CEBO created the figures. ABL, ASF, CEBO, GMW, HVS and YC analysed and interpreted the data. CEBO wrote the manuscript, and all authors edited the manuscript.


## Acknowledgements

The authors would like to thank Jocelyn Darby and Alana De Luca for assistance in the lab, Terry Pinfold for assistance in flow cytometry, and Amanda Patchett for assistance in bioinformatic analysis. We wish to thank G. Ralph for ongoing care of Tasmanian devils, the Bonorong Wildlife Sanctuary for providing access to Tasmanian devils, and R. Pye for providing care for devils and collecting blood samples.


## References


Anders, S., Huber, W., 2010. Differential expression analysis for sequence count data. Genome Biol. 11, R106. https://doi.org/10.1186/gb-2010-11-10-r106

Andersen, L.C., Beaty, J.S., Nettles, J.W., Seyfried, C.E., Nepom, G.T., Nepom, B.S., 1991. Allelic polymorphism in transcriptional regulatory regions of HLA-DQB genes. J. Exp. Med. 173, 181–192. https://doi.org/10.1084/jem.173.1.181

Andrews, S., 2010. FastQC: A Quality Control tool for High Throughput Sequence Data [WWW Document]. https://doi.org/https://www.bioinformatics.babraham.ac.uk/projects/fastqc/

Bennett, S.R.M., Carbone, F.R., Karamalis, F., Flavell, R.A., Miller, J.F.A.P., Heath, W.R., 1998. Help for cytotoxic-T-cell responses is mediated by CD4O signalling. Nature 393, 478–480. https://doi.org/10.1038/30996

Bullard, J.H., Purdom, E., Hansen, K.D., Dudoit, S., 2010. Evaluation of statistical methods for normalization and differential expression in mRNA-Seq experiments. BMC Bioinformatics 11, 94. https://doi.org/10.1186/1471-2105-11-94

Caldwell, A., Coleby, R., Tovar, C., Stammnitz, M.R., Kwon, Y.M., Owen, R.S., Tringides, M., Murchison, E.P., Skjødt, K., Thomas, G.J., Kaufman, J., Elliott, T., Woods, G.M., Siddle, H.V., 2018. The newly-arisen Devil facial tumour disease 2 (DFT2) reveals a mechanism for the emergence of a contagious cancer. Elife 7, e35314. https://doi.org/10.7554/eLife.35314

Caplen, H.S., Salvadori, S., Gansbacher, B., Zier, K.S., 1992. Post-transcriptional regulation of MHC class II expression in human T cells. Cell. Immunol. 139, 98–107. https://doi.org/10.1016/0008-8749(92)90103-V

Carrel, S., Schmidt-Kessen, A., Giuffrè, L., 1985. Recombinant interferon-γ can induce the expression of HLA-DR and -DC on DR-negative melanoma cells and enhance the expression of HLA-ABC and tumor-associated antigens. Eur. J. Immunol. 15, 118–123. https://doi.org/10.1002/eji.1830150204

Cheng, Y., Stuart, A., Morris, K., Taylor, R., Siddle, H., Deakin, J., Jones, M., Amemiya, C.T., Belov, K., 2012. Antigen-presenting genes and genomic copy number variations in the Tasmanian devil MHC. BMC Genomics 13, 87. https://doi.org/10.1186/1471-2164-13-87

Cunningham, C.X., Comte, S., McCallum, H., Hamilton, D.G., Hamede, R., Storfer, A., Hollings, T., Ruiz-Aravena, M., Kerlin, D.H., Brook, B.W., Hocking, G., Jones, M.E., 2021. Quantifying 25 years of disease-caused declines in Tasmanian devil populations: host density drives spatial pathogen spread. Ecol. Lett. 24, 958–969. https://doi.org/10.1111/ele.13703

Dalloul, A.H., Chmouzis, E., Ngo, K., Fung-Leung, W.P., 1996. Adoptively transferred CD4+ lymphocytes from CD8 -/- mice are sufficient to mediate the rejection of MHC class II or class I disparate skin grafts. J. Immunol. 156, 4114–4119.

Ekkirala, C.R., Cappello, P., Accolla, R.S., Giovarelli, M., Romero, I., Garrido, C., Garcia-Lora, A.M., Novelli, F., 2014. Class II Transactivator-Induced MHC Class II Expression in Pancreatic Cancer Cells Leads to Tumor Rejection and a Specific Antitumor Memory Response. Pancreas 43, 1066–1072. https://doi.org/10.1097/MPA.0000000000000160

Flies, A.S., Darby, J.M., Murphy, P.R., Pinfold, T.L., Patchett, A.L., Lennard, P.R., 2020. Generation and Testing of Fluorescent Adaptable Simple Theranostic (FAST) Proteins. Bio-protocol 10, e3696. https://doi.org/10.21769/BioProtoc.3696

Flies, A.S., Lyons, A.B., Corcoran, L.M., Papenfuss, A.T., Murphy, J.M., Knowles, G.W., Woods, G.M., Hayball, J.D., 2016. PD-L1 is not constitutively expressed on Tasmanian devil facial tumor cells but is strongly upregulated in response to IFN-γ and can be expressed in the tumor microenvironment. Front. Immunol. 7, 581. https://doi.org/10.3389/fimmu.2016.00581

Frangione, V., Mortara, L., Castellani, P., De Lerma Barbaro, A., Accolla, R.S., 2010. CIITA-driven MHC-II positive tumor cells: Preventive vaccines and superior generators of antitumor $CD4^+$ T lymphocytes for immunotherapy. Int. J. Cancer 127, 1614–1624. https://doi.org/10.1002/ijc.25183

Gobin, S.J.P., Peijnenburg, A., Keijsers, V., Van Den Elsen, P.J., 1997. Site α is crucial for two routes of IFNγ-induced MHC class I transactivation: the ISRE-mediated route and a novel pathway involving CIITA. Immunity 6, 601–611. https://doi.org/10.1016/S1074-7613(00)80348-9

Gobin, S.J.P., van Zutphen, M., Westerheide, S.D., Boss, J.M., van den Elsen, P.J., 2001. The MHC-specific enhanceosome and its role in MHC class I and $\beta_2$-microglobulin gene transactivation. J. Immunol. 167, 5175–5184. https://doi.org/10.4049/jimmunol.167.9.5175

Gu, Z., Eils, R., Schlesner, M., 2016. Complex heatmaps reveal patterns and correlations in multidimensional genomic data. Bioinformatics 32, 2847–2849.

https://doi.org/10.1093/bioinformatics/btw313

Hawkins, C.E., Baars, C., Hesterman, H., Hocking, G.J., Jones, M.E., Lazenby, B., Mann, D., Mooney, N., Pemberton, D., Pyecroft, S., Restani, M., Wiersma, J., 2006. Emerging disease and population decline of an island endemic, the Tasmanian devil Sarcophilus harrisii. Biol. Conserv. 131, 307–324. https://doi.org/10.1016/J.BIOCON.2006.04.010

Hirsch, M.R., Wietzerbin, J., Pierres, M., Goridis, C., 1983. Expression of Ia antigens by cultured astrocytes treated with gamma-interferon. Neurosci. Lett. 41, 199–204. https://doi.org/10.1016/0304-3940(83)90247-1

Howson, L.J., Morris, K.M., Kobayashi, T., Tovar, C., Kreiss, A., Papenfuss, A.T., Corcoran, L., Belov, K., Woods, G.M., 2014. Identification of dendritic cells, B cell and T cell subsets in Tasmanian devil lymphoid tissue; evidence for poor immune cell infiltration into devil facial tumors. Anat. Rec. (Hoboken). 297, 925–938. https://doi.org/10.1002/ar.22904

Huang, D.W., Sherman, B.T., Lempicki, R.A., 2009a. Bioinformatics enrichment tools: Paths toward the comprehensive functional analysis of large gene lists. Nucleic Acids Res. 37, 1–13. https://doi.org/10.1093/nar/gkn923

Huang, D.W., Sherman, B.T., Lempicki, R.A., 2009b. Systematic and integrative analysis of large gene lists using DAVID bioinformatics resources. Nat. Protoc. 4, 44–57. https://doi.org/10.1038/nprot.2008.211

Hung, K., Hayashi, R., Lafond-Walker, A., Lowenstein, C., Pardoll, D., Levitsky, H., 1998. The central role of CD4+ T cells in the antitumor immune response. J. Exp. Med. 188, 2357–2368. https://doi.org/10.1084/jem.188.12.2357

Janssen, E.M., Lemmens, E.E., Wolfe, T., Christen, U., Von Herrath, M.G., Schoenberger, S.P., 2003. CD4+ T cells are required for secondary expansion and memory in CD8+ T lymphocytes. Nature 421, 852–856. https://doi.org/10.1038/nature01441

Kowarz, E., Löscher, D., Marschalek, R., 2015. Optimized Sleeping Beauty transposons rapidly generate stable transgenic cell lines. Biotechnol. J. 10, 647–653. https://doi.org/10.1002/biot.201400821

Krieger, N.R., Yin, D.P., Fathman, C.G., 1996. CD4+ but not CD8+ cells are essential for allorejection. J. Exp. Med. 184, 2013–2018. https://doi.org/10.1084/jem.184.5.2013

Kulkarni, S., Savan, R., Qi, Y., Gao, X., Yuki, Y., Bass, S.E., Martin, M.P., Hunt, P., Deeks, S.G., Telenti, A., Pereyra, F., Goldstein, D., Wolinsky, S., Walker, B., Young, H.A., Carrington, M., 2011. Differential microRNA regulation of HLA-C expression and its association with HIV control. Nature 472, 495–498. https://doi.org/10.1038/nature09914

Kumamoto, Y., Mattei, L.M., Sellers, S., Payne, G.W., Iwasaki, A., 2011. CD4+ T cells support cytotoxic T lymphocyte priming by controlling lymph node input. Proc. Natl. Acad. Sci. U. S. A. 108, 8749–8754. https://doi.org/10.1073/pnas.1100567108

Law, C.W., Chen, Y., Shi, W., Smyth, G.K., 2014. voom: Precision weights unlock linear model analysis tools for RNA-seq read counts. Genome Biol. 15, R29. https://doi.org/10.1186/gb-2014-15-2-r29

Lazenby, B.T., Tobler, M.W., Brown, W.E., Hawkins, C.E., Hocking, G.J., Hume, F., Huxtable, S., Iles, P., Jones, M.E., Lawrence, C., Thalmann, S., Wise, P., Williams, H., Fox, S., Pemberton, D., 2018. Density trends and demographic signals uncover the long-term impact of transmissible cancer in Tasmanian devils. J. Appl. Ecol. 55, 1368–1379.

https://doi.org/10.1111/1365-2664.13088

Leen, M.P.J.M., Gorski, J., 1996. Differential expression of isomorphic HLA-DRβ genes is not a sole function of transcription. Hum. Immunol. 50, 111–120. https://doi.org/10.1016/0198-8859(96)00154-1

Liao, Y., Smyth, G.K., Shi, W., 2014. featureCounts: an efficient general purpose program for assigning sequence reads to genomic features. Bioinformatics 30, 923–930. https://doi.org/10.1093/bioinformatics/btt656

Liao, Y., Smyth, G.K., Shi, W., 2013. The Subread aligner: fast, accurate and scalable read mapping by seed-and-vote. Nucleic Acids Res. 41, e108–e108. https://doi.org/10.1093/nar/gkt214

Martin, B.K., Chin, K.C., Olsen, J.C., Skinner, C.A., Dey, A., Ozato, K., Ting, J.P.Y., 1997. Induction of MHC class I expression by the MHC class II transactivator CIITA. Immunity 6, 591–600. https://doi.org/10.1016/S1074-7613(00)80347-7

Masternak, K., Muhlethaler-Mottet, A., Villard, J., Zufferey, M., Steimle, V., Reith, W., 2000. CIITA is a transcriptional coactivator that is recruited to MHC class II promoters by multiple synergistic interactions with an enhanceosome complex. Genes Dev. 14, 1156–1166. https://doi.org/10.1101/gad.14.9.1156

Mátés, L., Chuah, M.K.L., Belay, E., Jerchow, B., Manoj, N., Acosta-Sanchez, A., Grzela, D.P., Schmitt, A., Becker, K., Matrai, J., Ma, L., Samara-Kuko, E., Gysemans, C., Pryputniewicz, D., Miskey, C., Fletcher, B., VandenDriessche, T., Ivics, Z., Izsvák, Z., 2009. Molecular evolution of a novel hyperactive Sleeping Beauty transposase enables robust stable gene transfer in vertebrates. Nat. Genet. 41, 753–761. https://doi.org/10.1038/ng.343

Meazza, R., Comes, A., Orengo, A.M., Ferrini, S., Accolla, R.S., 2003. Tumor rejection by gene transfer of the MHC class II transactivator in murine mammary adenocarcinoma cells. Eur. J. Immunol. 33, 1183–1192. https://doi.org/10.1002/eji.200323712

Meissner, T.B., Liu, Y.-J., Lee, K.-H., Li, A., Biswas, A., van Eggermond, M.C.J.A., van den Elsen, P.J., Kobayashi, K.S., 2012. NLRC5 cooperates with the RFX transcription factor complex to induce MHC class I gene expression. J. Immunol. 188, 4951–4958. https://doi.org/10.4049/jimmunol.1103160

Meyer zu Hörste, G., Heidenreich, H., Lehmann, H.C., Ferrone, S., Hartung, H.P., Wiendl, H., Kieseier, B.C., 2010a. Expression of antigen processing and presenting molecules by Schwann cells in inflammatory neuropathies. Glia 58, 80–92. https://doi.org/10.1002/glia.20903

Meyer zu Hörste, G., Heidenreich, H., Mausberg, A.K., Lehmann, H.C., ten Asbroek, A.L.M.A., Saavedra, J.T., Baas, F., Hartung, H.P., Wiendl, H., Kieseier, B.C., 2010b. Mouse Schwann cells activate MHC class I and II restricted T-cell responses, but require external peptide processing for MHC class II presentation. Neurobiol. Dis. 37, 483–490. https://doi.org/10.1016/j.nbd.2009.11.006

Mortara, L., Frangione, V., Castellani, P., De Lerma Barbaro, A., Accolla, R.S., 2009. Irradiated CIITA-positive mammary adenocarcinoma cells act as a potent anti-tumor-preventive vaccine by inducing tumor-specific $CD4^+$ T cell priming and $CD8^+$ T cell effector functions. Int. Immunol. 21, 655–665. https://doi.org/10.1093/intimm/dxp034

Murchison, E.P., Tovar, C., Hsu, A., Bender, H.S., Kheradpour, P., Rebbeck, C.A., Obendorf, D., Conlan, C., Bahlo, M., Blizzard, C.A., Pyecroft, S., Kreiss, A., Kellis, M., Stark, A.,

Harkins, T.T., Marshall Graves, J.A., Woods, G.M., Hannon, G.J., Papenfuss, A.T., 2010. The Tasmanian devil transcriptome reveals Schwann cell origins of a clonally transmissible cancer. Science 327, 84–87. https://doi.org/10.1126/science.1180616

Oliveros, J.C., 2015. Venny. An interactive tool for comparing lists with Venn's diagrams. [WWW Document]. URL https://bioinfogp.cnb.csic.es/tools/venny/index.html

Ong, C.E.B., Patchett, A.L., Darby, J.M., Chen, J., Liu, G.-S., Lyons, A.B., Woods, G.M., Flies, A.S., 2021. NLRC5 regulates expression of MHC-I and provides a target for anti-tumor immunity in transmissible cancers. J. Cancer Res. Clin. Oncol. 1–19. https://doi.org/10.1007/s00432-021-03601-x

Ostrand-Rosenberg, S., 2005. CD4+ T lymphocytes: A critical component of antitumor immunity. Cancer Invest. https://doi.org/10.1081/CNV-67428

Ostrand-Rosenberg, S., Clements, V.K., Thakur, A., Cole, G.A., 1989. Transfection of major histocompatibility complex class I and class II genes causes tumour rejection. Int. J. Immunogenet. 16, 343–349. https://doi.org/10.1111/j.1744-313X.1989.tb00481.x

Ostrand-Rosenberg, S., Thakur, A., Clements, V., 1990. Rejection of mouse sarcoma cells after transfection of MHC class II genes. J. Immunol. 144, 4068–4071.

Otten, L.A., Steimle, V., Bontron, S., Mach, B., 1998. Quantitative control of MHC class II expression by the transactivator CIITA. Eur. J. Immunol. 28, 473–478. https://doi.org/10.1002/(SICI)1521-4141(199802)28:02

Patchett, A.L., Coorens, T.H.H., Darby, J., Wilson, R., McKay, M.J., Kamath, K.S., Rubin, A., Wakefield, M., Mcintosh, L., Mangiola, S., Pye, R.J., Flies, A.S., Corcoran, L.M., Lyons, A.B., Woods, G.M., Murchison, E.P., Papenfuss, A.T., Tovar, C., 2020. Two of a kind: transmissible Schwann cell cancers in the endangered Tasmanian devil (*Sarcophilus harrisii*). Cell. Mol. Life Sci. 77, 1847–1858. https://doi.org/10.1007/s00018-019-03259-2

Patchett, A.L., Wilson, R., Charlesworth, J.C., Corcoran, L.M., Papenfuss, A.T., Lyons, B.A., Woods, G.M., Tovar, C., 2018. Transcriptome and proteome profiling reveals stress-induced expression signatures of imiquimod-treated Tasmanian devil facial tumor disease (DFTD) cells. Oncotarget 9, 15895–15914. https://doi.org/10.18632/oncotarget.24634

Pearse, A.-M., Swift, K., 2006. Allograft theory: Transmission of devil facial-tumour disease. Nature 439, 549. https://doi.org/10.1038/439549a

Pearse, A.-M., Swift, K., Hodson, P., Hua, B., McCallum, H., Pyecroft, S., Taylor, R., Eldridge, M.D.B., Belov, K., 2012. Evolution in a transmissible cancer: a study of the chromosomal changes in devil facial tumor (DFT) as it spreads through the wild Tasmanian devil population. Cancer Genet. 205, 101–112. https://doi.org/10.1016/j.cancergen.2011.12.001

Phipson, B., Lee, S., Majewski, I.J., Alexander, W.S., Smyth, G.K., 2016. Robust hyperparameter estimation protects against hypervariable genes and improves power to detect differential expression. Ann. Appl. Stat. 10, 946–963. https://doi.org/10.1214/16-AOAS920

Pietra, B.A., Wiseman, A., Bolwerk, A., Rizeq, M., Gill, R.G., 2000. CD4 T cell-mediated cardiac allograft rejection requires donor but not host MHC class II. J. Clin. Invest. 106, 1003–1010. https://doi.org/10.1172/JCI10467

Propper, D.J., Chao, D., Braybrooke, J.P., Bahl, P., Thavasu, P., Balkwill, F., Turley, H., Dobbs, N., Gatter, K., Talbot, D.C., Harris, A.L., Ganesan, T.S., 2003. Low-Dose IFN-γ Induces Tumor MHC Expression in Metastatic Malignant Melanoma. Clin. Cancer Res. 9, 84–92.

Pye, R., Darby, J., Flies, A., Fox, S., Carver, S., Elmer, J., Swift, K., Hogg, C., Pemberton, D., Woods, G., Lyons, A.B., n.d. Post release immune responses of Tasmanian devils vaccinated with an experimental devil facial tumour disease vaccine. Wildl. Res.

Pye, R., Hamede, R., Siddle, H. V., Caldwell, A., Knowles, G.W., Swift, K., Kreiss, A., Jones, M.E., Lyons, A.B., Woods, G.M., 2016a. Demonstration of immune responses against devil facial tumour disease in wild Tasmanian devils. Biol. Lett. 12, 20160553. https://doi.org/10.1098/RSBL.2016.0553

Pye, R.J., Pemberton, D., Tovar, C., Tubio, J.M.C., Dun, K.A., Fox, S., Darby, J., Hayes, D., Knowles, G.W., Kreiss, A., Siddle, H.V.T., Swift, K., Lyons, A.B., Murchison, E.P., Woods, G.M., 2016b. A second transmissible cancer in Tasmanian devils. Proc. Natl. Acad. Sci. U. S. A. 113, 374–379. https://doi.org/10.1073/pnas.1519691113

R Core Team, 2020. R: A Language and Environment for Statistical Computing.

Risso, D., Schwartz, K., Sherlock, G., Dudoit, S., 2011. GC-Content Normalization for RNA-Seq Data. BMC Bioinformatics 12, 480. https://doi.org/10.1186/1471-2105-12-480

Ritchie, M.E., Phipson, B., Wu, D., Hu, Y., Law, C.W., Shi, W., Smyth, G.K., 2015. *limma* powers differential expression analyses for RNA-sequencing and microarray studies. Nucleic Acids Res. 43, e47. https://doi.org/10.1093/nar/gkv007

Robinson, M.D., McCarthy, D.J., Smyth, G.K., 2009. edgeR: A Bioconductor package for differential expression analysis of digital gene expression data. Bioinformatics 26, 139–140. https://doi.org/10.1093/bioinformatics/btp616

Robinson, M.D., Oshlack, A., 2010. A scaling normalization method for differential expression analysis of RNA-seq data. Genome Biol. 11, R25. https://doi.org/10.1186/gb-2010-11-3-r25

RStudio Team, 2020. RStudio: Integrated Development Environment for R.

Siddle, H. V, Kreiss, A., Eldridge, M.D.B., Noonan, E., Clarke, C.J., Pyecroft, S., Woods, G.M., Belov, K., 2007. Transmission of a fatal clonal tumor by biting occurs due to depleted MHC diversity in a threatened carnivorous marsupial. Proc. Natl. Acad. Sci. U. S. A. 104, 16221–6. https://doi.org/10.1073/pnas.0704580104

Siddle, H. V, Kreiss, A., Tovar, C., Yuen, C.K., Cheng, Y., Belov, K., Swift, K., Pearse, A.-M., Hamede, R., Jones, M.E., Skjødt, K., Woods, G.M., Kaufman, J., 2013. Reversible epigenetic down-regulation of MHC molecules by devil facial tumour disease illustrates immune escape by a contagious cancer. Proc. Natl. Acad. Sci. U. S. A. 110, 5103–5108. https://doi.org/10.1073/pnas.1219920110

Stammnitz, M.R., Coorens, T.H.H., Gori, K.C., Hayes, D., Fu, B., Wang, J., Martin-Herranz, D.E., Alexandrov, L.B., Baez-Ortega, A., Barthorpe, S., Beck, A., Giordano, F., Knowles, G.W., Kwon, Y.M., Hall, G., Price, S., Pye, R.J., Tubio, J.M.C., Siddle, H.V.T., Sohal, S.S., Woods, G.M., McDermott, U., Yang, F., Garnett, M.J., Ning, Z., Murchison, E.P., 2018. The Origins and Vulnerabilities of Two Transmissible Cancers in Tasmanian Devils. Cancer Cell 33, 607-619.e15. https://doi.org/10.1016/J.CCELL.2018.03.013

Steimle, V., Otten, L.A., Zufferey, M., Mach, B., 1993. Complementation cloning of an MHC class II transactivator mutated in hereditary MHC class II deficiency (or bare lymphocyte syndrome). Cell 75, 135–146. https://doi.org/10.1016/S0092-8674(05)80090-X

Steimle, V., Siegrist, C.A., Mottet, A., Lisowska-Grospierre, B., Mach, B., 1994. Regulation of MHC class II expression by interferon-γ mediated by the transactivator gene CIITA. Science (80-. ). 265, 106–109. https://doi.org/10.1126/science.8016643

Tay, R.E., Richardson, E.K., Toh, H.C., 2020. Revisiting the role of CD4+ T cells in cancer immunotherapy—new insights into old paradigms. Cancer Gene Ther. https://doi.org/10.1038/s41417-020-0183-x

Tovar, C., Pye, R.J., Kreiss, A., Cheng, Y., Brown, G.K., Darby, J., Malley, R.C., Siddle, H.V.T., Skjødt, K., Kaufman, J., Silva, A., Baz Morelli, A., Papenfuss, A.T., Corcoran, L.M., Murphy, J.M., Pearse, M.J., Belov, K., Lyons, A.B., Woods, G.M., 2017. Regression of devil facial tumour disease following immunotherapy in immunised Tasmanian devils. Sci. Rep. 7, 43827. https://doi.org/10.1038/srep43827

# Tables

Table 1. List of all devil facial tumour (DFT) cell lines and treatments

| ID # | Sample name | Parent cell line | Treatment | References | ENA project # |
|---|---|---|---|---|---|
| 1 | DFT1.WT | DFT1 C5065 | Untreated | Patchett et al., (2018) | PRJNA416378 |
| 2 | DFT2.WT$^{RV}$ | DFT2 RV | Untreated | Patchett et al., (2020) | PRJEB28680 |
| 3 | DFT2.WT | DFT2 JV | Untreated | Ong et al., (2021) | PRJEB39847 |
| 4 | DFT1.WT + IFNG | DFT1 C5065 | 5 ng/mL IFNG, 24h | Ong et al., (2021) | PRJEB39847 |
| 5 | DFT2.WT$^{RV}$ + IFNG | DFT2 RV | 5 ng/mL IFNG, 24h | Ong et al., (2021) | PRJEB39847 |
| 6 | DFT1.BFP | DFT1 C5065 | Transfected with empty vector pSBbi-BH | Ong et al., (2021) | PRJEB39847 |
| 7 | DFT2.BFP | DFT2 JV | Transfected with empty vector pSBbi-BH | Ong et al., (2021) | PRJEB39847 |
| 8 | DFT1.NLRC5 | DFT1 C5065 | Transfected with NLRC5 vector pCO1 | Ong et al., (2021) | PRJEB39847 |
| 9 | DFT2.NLRC5 | DFT2 JV | Transfected with NLRC5 vector pCO1 | Ong et al., (2021) | PRJEB39847 |
| 10 | DFT1.CIITA | DFT1 C5065 | Transfected with CIITA vector pCO2 | This study | PRJEB45867 |
| 11 | DFT2.CIITA | DFT2 JV | Transfected with CIITA vector pCO2 | This study | PRJEB45867 |

Table 2. Top 20 most significantly upregulated genes in DFT1.CIITA

| Gene | Gene description | MHC pathway | $log_2FC$ | FDR |
|---|---|---|---|---|
| *SAHA-DAA* | Class II histocompatibility antigen, DA alpha chain | Class II | 17.09 | 1.90E-04 |
| *CD74* | CD74 molecule | Class II | 16.39 | 7.77E-05 |
| *CIITA* | Class II major histocompatibility complex transactivator | Class II | 15.40 | 1.07E-04 |
| *SAHA-DMB* | Class II histocompatibility antigen, DM beta chain | Class II | 10.26 | 7.00E-05 |
| *SAHA-DAB_X2* | Class II histocompatibility antigen, DA beta chain | Class II | 9.04 | 1.11E-03 |
| *SAHA-DAB_X1* | Class II histocompatibility antigen, DA beta chain | Class II | 8.82 | 7.77E-04 |
| *PSMB9* | Proteasome 20S subunit beta 9 | Class I | 8.52 | 4.08E-04 |
| *SAHA-DMA* | Class II histocompatibility antigen, DM alpha chain | Class II | 6.52 | 5.12E-04 |
| *TAP1* | Transporter 1, ATP binding cassette subfamily B member | Class I | 6.46 | 6.95E-04 |
| *PSMB8* | Proteasome 20S subunit beta 8 | Class I | 6.13 | 1.29E-03 |
| *SAHA-DAB3* | Class II histocompatibility antigen, DA beta chain | Class II | 6.08 | 7.72E-05 |
| *SAHA-UC* | Class I histocompatibility antigen heavy chain | Class I | 5.08 | 2.17E-03 |
| *SAHA-UA* | Class I histocompatibility antigen heavy chain | Class I | 4.77 | 2.29E-03 |
| *B2M* | Beta-2-microglobulin | Class I | 4.43 | 1.96E-05 |
| *SAHA-UB* | Class I histocompatibility antigen heavy chain | Class I | 4.41 | 2.25E-03 |
| *SAHA-DAB2* | Class II histocompatibility antigen, DA beta chain | Class II | 4.21 | 1.96E-05 |
| *ICOSLG* | Inducible T Cell Costimulator (ICOS) Ligand | Unrelated | 3.98 | 1.14E-03 |
| *KIF6* | Kinesin family member 6 | Unrelated | 3.88 | 1.10E-02 |
| *BARX1* | BARX homeobox 1 | Unrelated | 3.68 | 4.99E-03 |
| *MID1* | Midline 1 | Unrelated | 3.67 | 3.52E-03 |

*See **Supplementary Table 3** full list of differentially expressed genes and $log_2TPM$ values.*

Table 3. Significantly upregulated genes in DFT2.CIITA

| **Gene** | **Gene description** | **MHC pathway** | **$log_2FC$** | **FDR** |
|---|---|---|---|---|
| *CD74* | CD74 molecule | Class II | 13.60 | 6.69E-03 |
| *CIITA* | Class II major histocompatibility complex transactivator | Class II | 11.50 | 2.31E-03 |
| *SAHA-DAA* | Class II histocompatibility antigen, DA alpha chain | Class II | 8.52 | 2.31E-03 |
| *SAHA-DMB* | Class II histocompatibility antigen, DM beta chain | Class II | 8.34 | 2.81E-04 |
| *SAHA-DAB3* | Class II histocompatibility antigen, DA beta chain | Class II | 7.09 | 2.19E-03 |
| *SAHA-DMA* | Class II histocompatibility antigen, DM alpha chain | Class II | 6.82 | 6.82E-04 |
| *SAHA-DAB2* | Class II histocompatibility antigen, DA beta chain | Class II | 4.14 | 3.10E-04 |
| *BTN2A2* | Butyrophilin subfamily 2 member A2 | Unrelated | 3.49 | 3.54E-02 |
| *NDUFA4L2* | NDUFA4 mitochondrial complex associated like 2 | Unrelated | 2.83 | 2.72E-02 |

*See **Supplementary Table 3** full list of differentially expressed genes and $log_2TPM$ values.*

Table 4. GO biological processes enriched in differentially expressed genes in DFT1.CIITA and DFT2.CIITA

| GO ID | GO term | Count | Term size | Fold enrichment | *p* value | FDR |
|---|---|---|---|---|---|---|
| **DFT1.CIITA** | | | | | | |
| *Upregulated* | | | | | | |
| GO:0019882 | antigen processing and presentation | 8 | 42 | 86.09 | 1.34E-12 | 1.19E-09 |
| GO:0006955 | immune response | 9 | 518 | 7.85 | 4.75E-06 | 2.12E-03 |
| *Downregulated* | | | | | | |
| GO:0007155 | cell adhesion | 44 | 719 | 2.14 | 2.27E-06 | 4.48E-03 |
| GO:0022610 | biological adhesion | 44 | 721 | 2.13 | 2.44E-06 | 4.48E-03 |
| GO:0023052 | signaling | 113 | 2746 | 1.44 | 4.94E-06 | 6.05E-03 |
| GO:0044700 | single organism signaling | 111 | 2726 | 1.42 | 1.12E-05 | 1.02E-02 |
| GO:0007154 | cell communication | 112 | 2773 | 1.41 | 1.46E-05 | 1.07E-02 |
| **DFT2.CIITA** | | | | | | |
| *Upregulated* | | | | | | |
| GO:0019882 | antigen processing and presentation | 4 | 42 | 215.21 | 9.33E-08 | 3.90E-05 |
| GO:0006955 | immune response | 4 | 518 | 17.45 | 1.87E-04 | 3.91E-02 |

# Figures

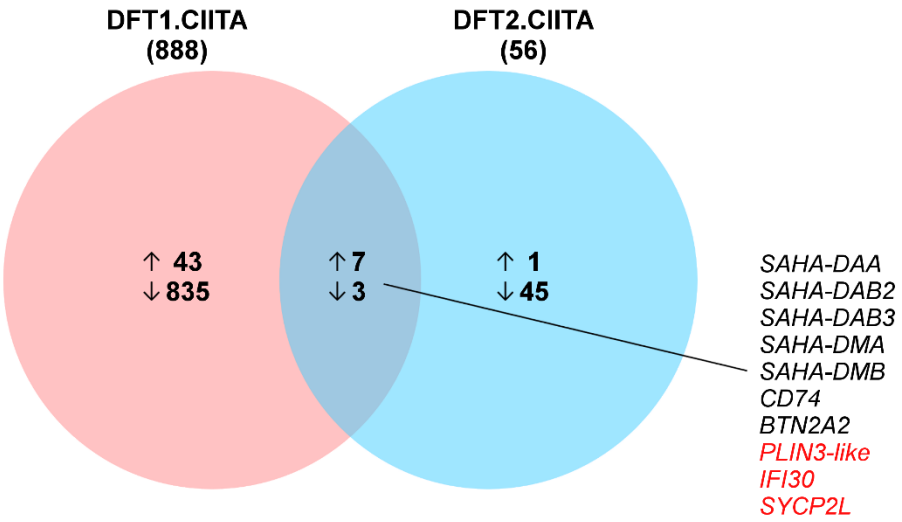


Fig. 1. Venn diagram of differentially expressed genes in DFT1 and DFT2 cells with CIITA overexpression. Change in gene expression was identified between DFT.CIITA and vector-only control DFT.BFP. Total number of DEGs is indicated in parenthesis under sample name and the number of upregulated (↑) and downregulated genes (↓) are described in each Venn circle. Mutually inclusive genes that were upregulated are indicated in black and downregulated in red.

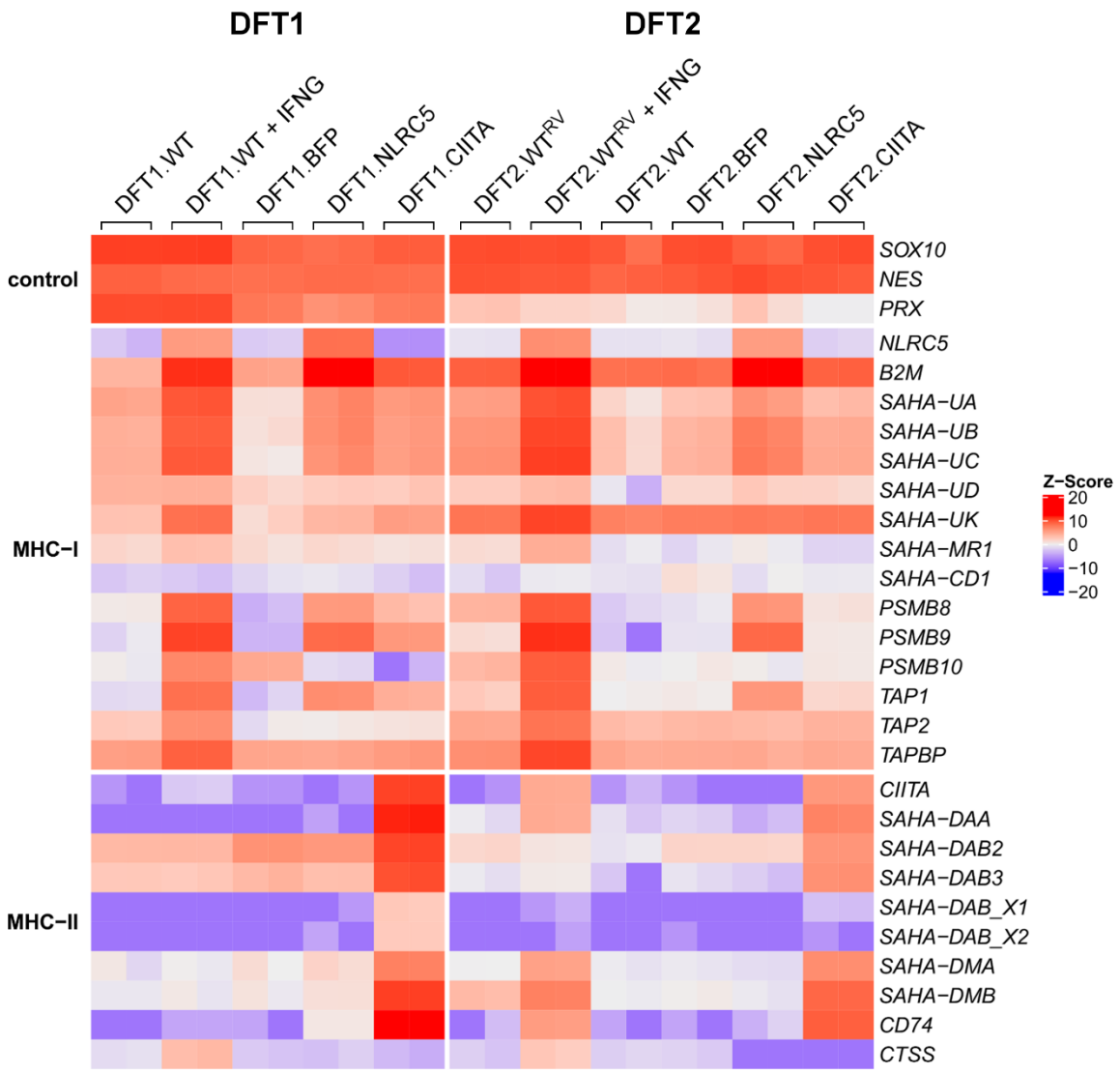


Fig. 2. Heatmap showing relative expression of genes involved in MHC-I and MHC-II antigen processing and presentation in wild type, IFNG-treated, BFP- (vector control), NLRC5-, and CIITA-expressing DFT1 and DFT2 cells. Z-scores were calculated from $\log_2$TPM expression values and scaled across each gene (rows). High and low relative expression are represented by red and blue, respectively. Replicates per treatment (*N*=2) are included in the heatmap.

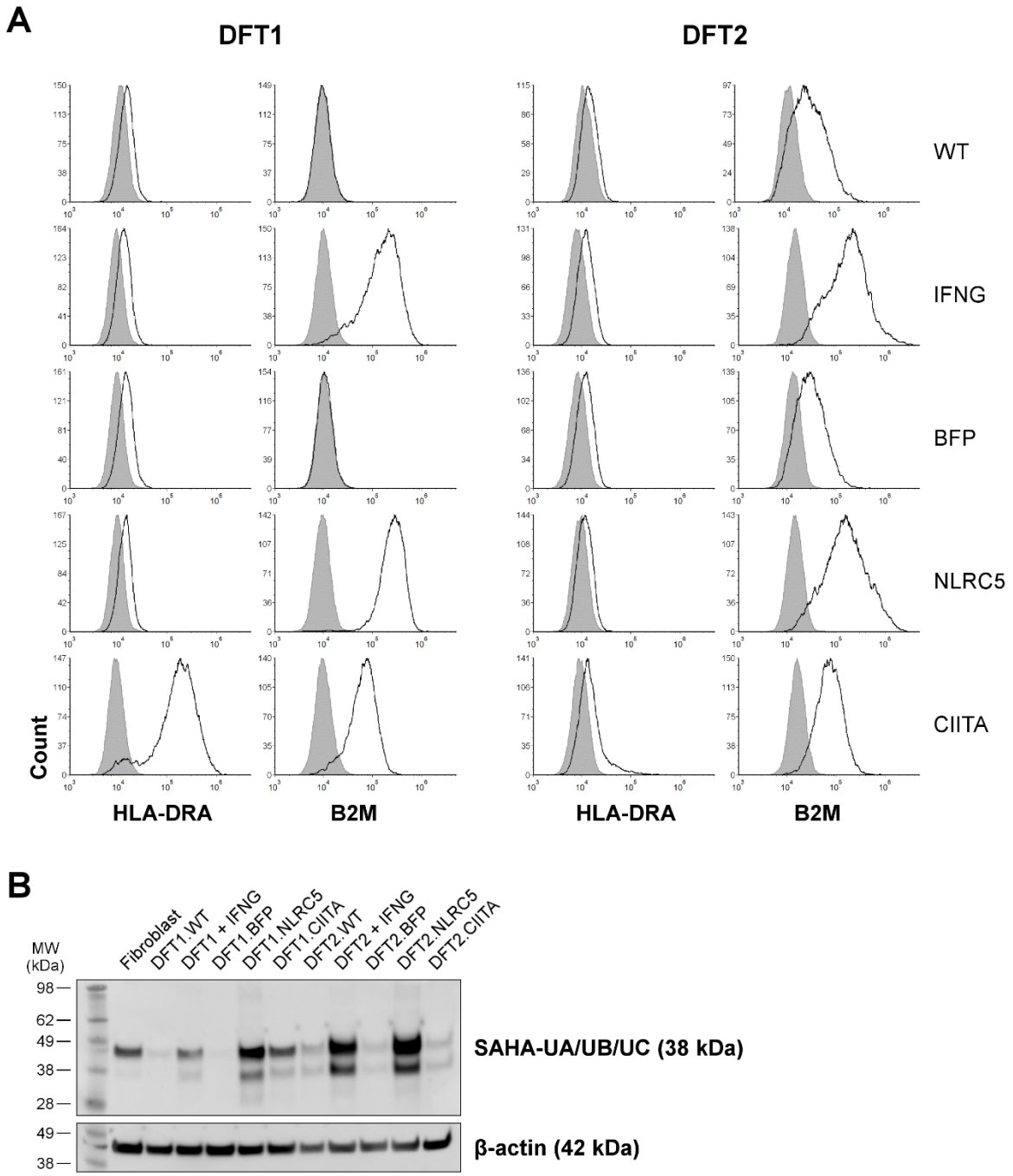


Fig. 3. Expression of MHC-II, B2M and MHC-I in DFT1 and DFT2 cell lines. (**A**) Wild type (WT), IFNG-treated (IFNG), vector-only control (BFP), NLRC5-overexpressing (NLRC5) or CIITA-overexpressing (CIITA) DFT1 and DFT2 cells were analysed by flow cytometry for B2M and MHC-II expression using antibodies against surface devil B2M or intracellular HLA-DR alpha chain (HLA-DRA), respectively (*solid line*). B2M and MHC-II expressions were overlaid with a secondary antibody-only control (*shaded area*). The results shown are representative of *N*=3 replicates/treatment. (**B**) Cell lysate from devil fibroblast, DFT1 and DFT2 cell lines was incubated with an antibody against MHC-I heavy chain genes SAHA-UA/UB/UC for western blot analysis of MHC-I expression. β-actin was included as a loading control. *MW*, molecular weight.

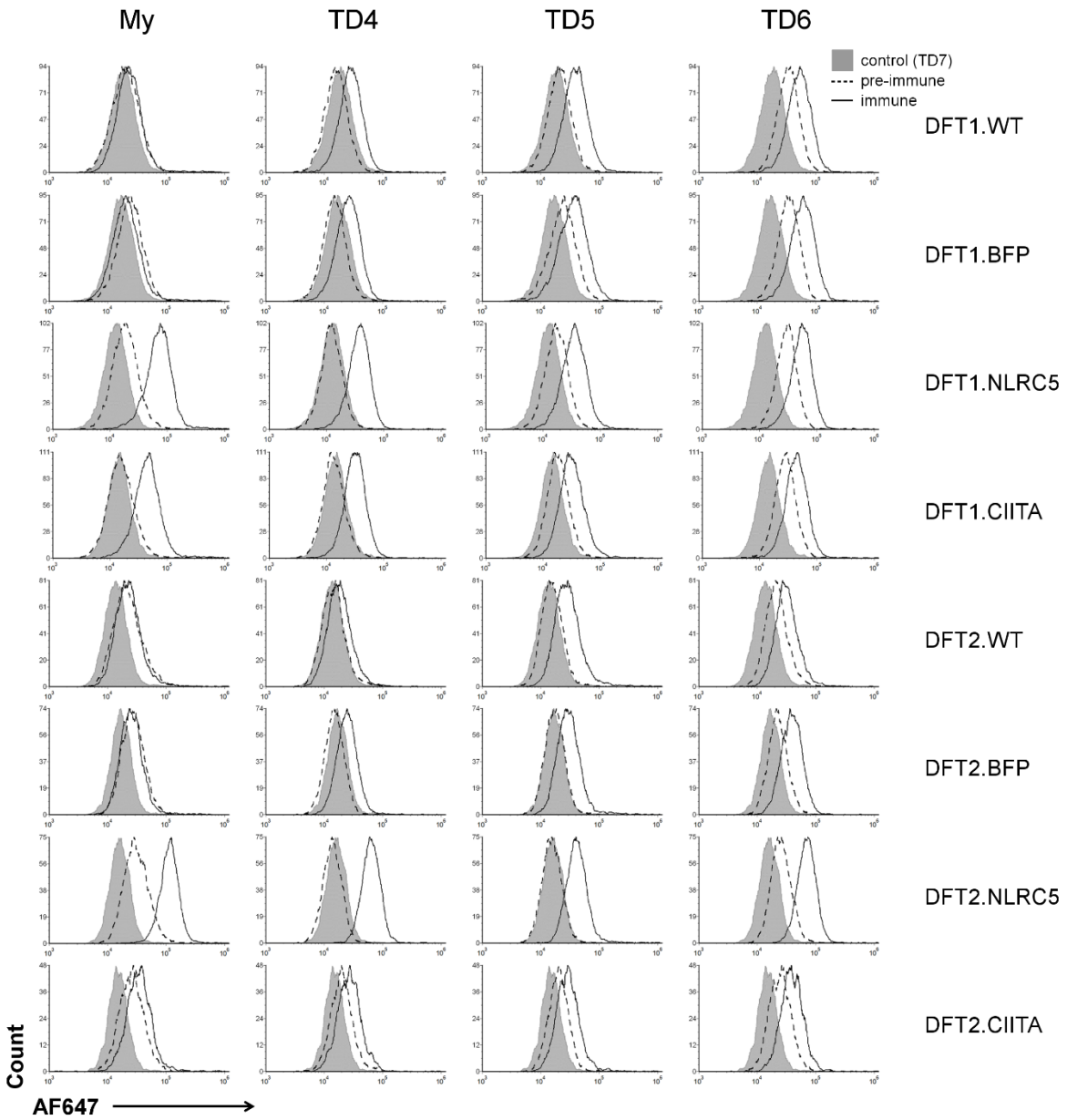


Fig. 4. Flow cytometric analysis of serum antibody response towards DFT1 and DFT2 cells overexpressing CIITA. Sera from four devils (My, TD4, TD5, TD6) with antibody responses to MHC-I$^{+}$ DFT1 cells after DFT1 infection (immune) were used. Antibody binding was compared against wild type (DFT.WT), vector-only (DFT.BFP) and NLRC5-overexpressing cells (DFT.NLRC5). Serum collected prior to infection (pre-immune) and from a non-infected devil (TD7) were included as negative controls. *AF647*, Alexa Fluor 647.

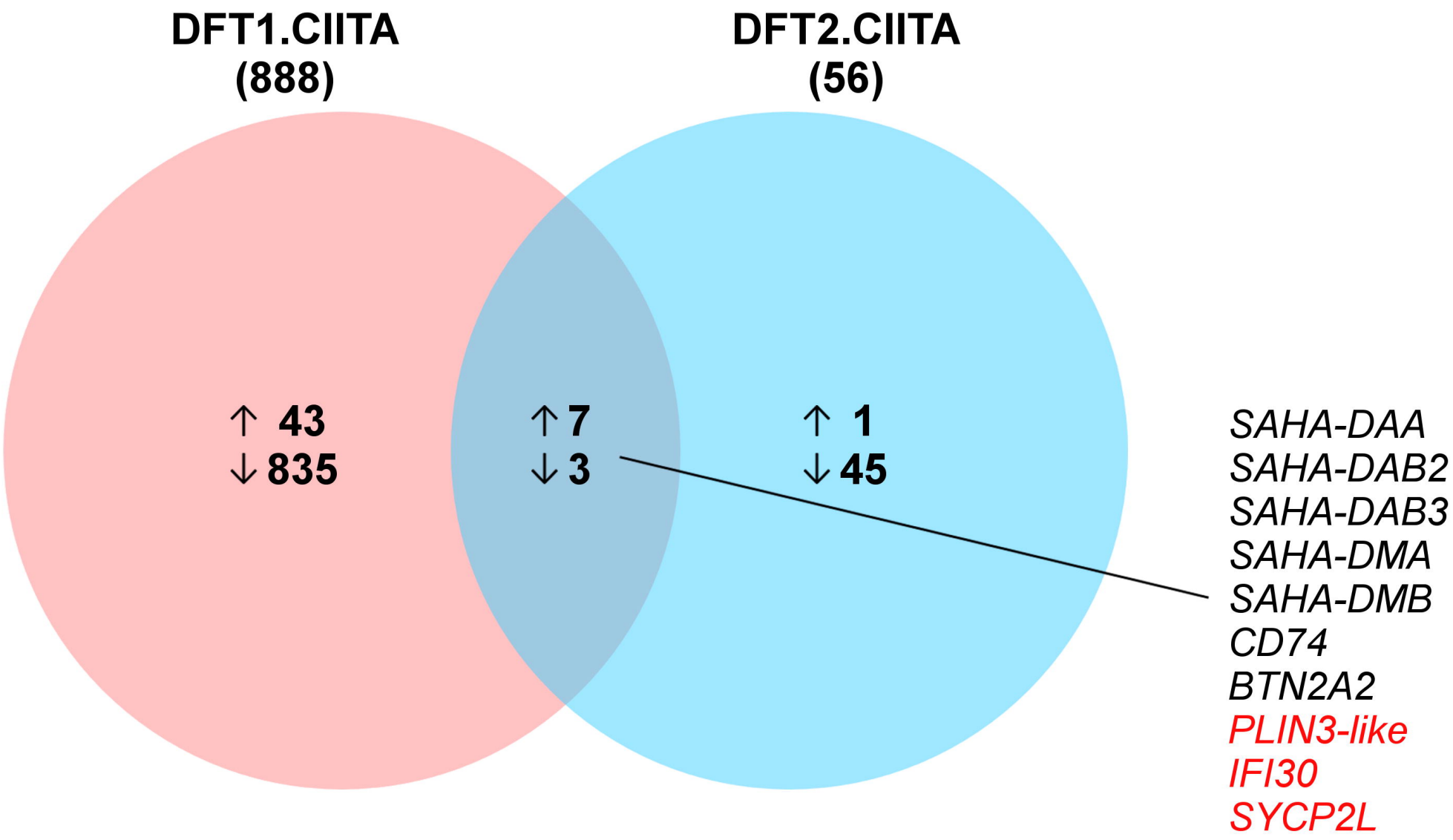
DFT1.CIITA
(888)
DFT2.CIITA
(56)
↑ 43
↓ 835
↑ 7
↓ 3
↑ 1
↓ 45
SAHA-DAA
SAHA-DAB2
SAHA-DAB3
SAHA-DMA
SAHA-DMB
CD74
BTN2A2
PLIN3-like
IFI30
SYCP2L

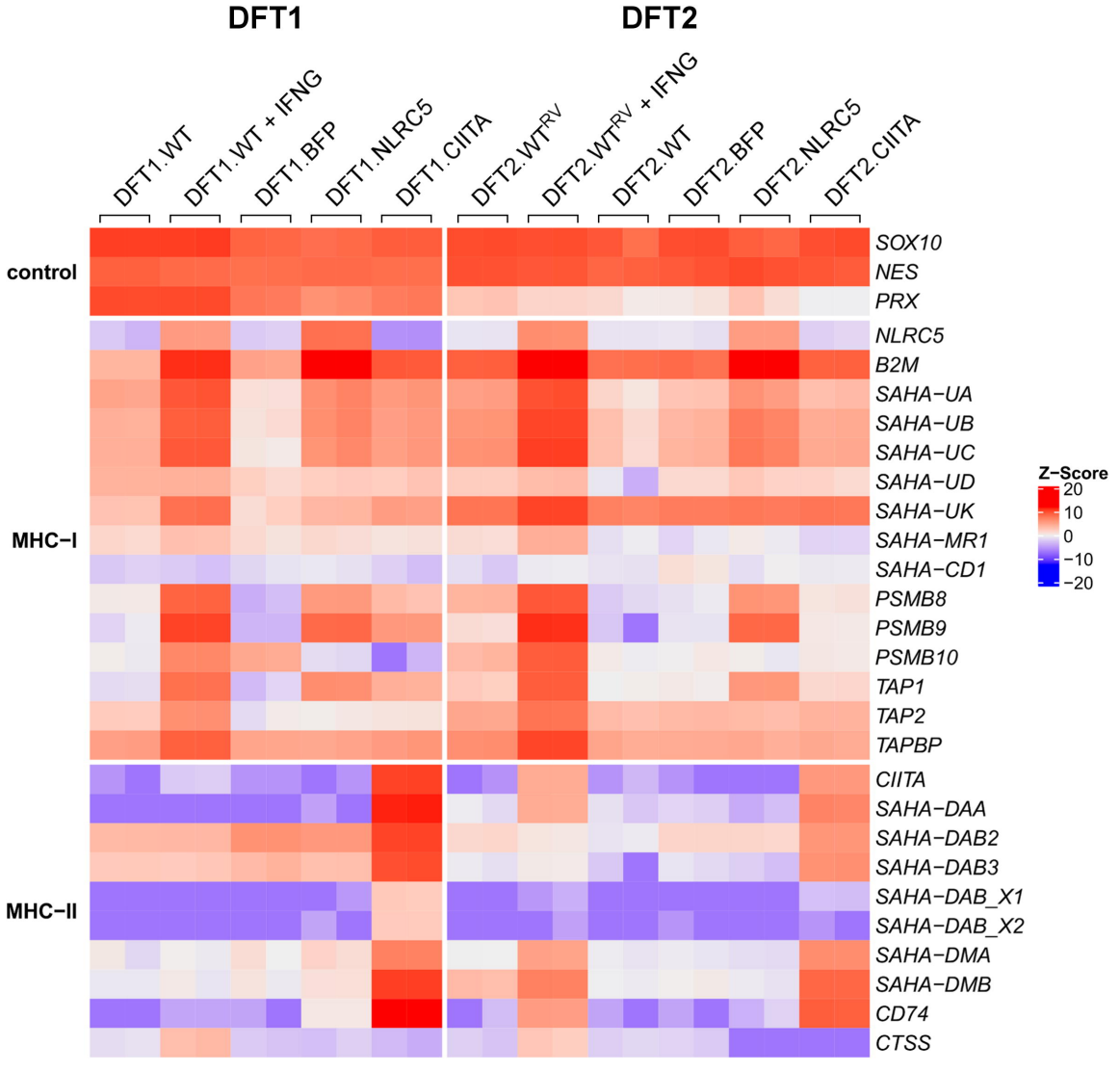
DFT1
DFT2
DFT1.WT
DFT1.WT + IFNG
DFT1.BFP
DFT1.NLRC5
DFT1.CIITA
DFT2.WT^RV
DFT2.WT^RV + IFNG
DFT2.WT
DFT2.BFP
DFT2.NLRC5
DFT2.CIITA
control
MHC−I
MHC−II
SOX10
NES
PRX
NLRC5
B2M
SAHA−UA
SAHA−UB
SAHA−UC
SAHA−UD
SAHA−UK
SAHA−MR1
SAHA−CD1
PSMB8
PSMB9
PSMB10
TAP1
TAP2
TAPBP
CIITA
SAHA−DAA
SAHA−DAB2
SAHA−DAB3
SAHA−DAB_X1
SAHA−DAB_X2
SAHA−DMA
SAHA−DMB
CD74
CTSS
Z−Score
20
10
0
−10
−20

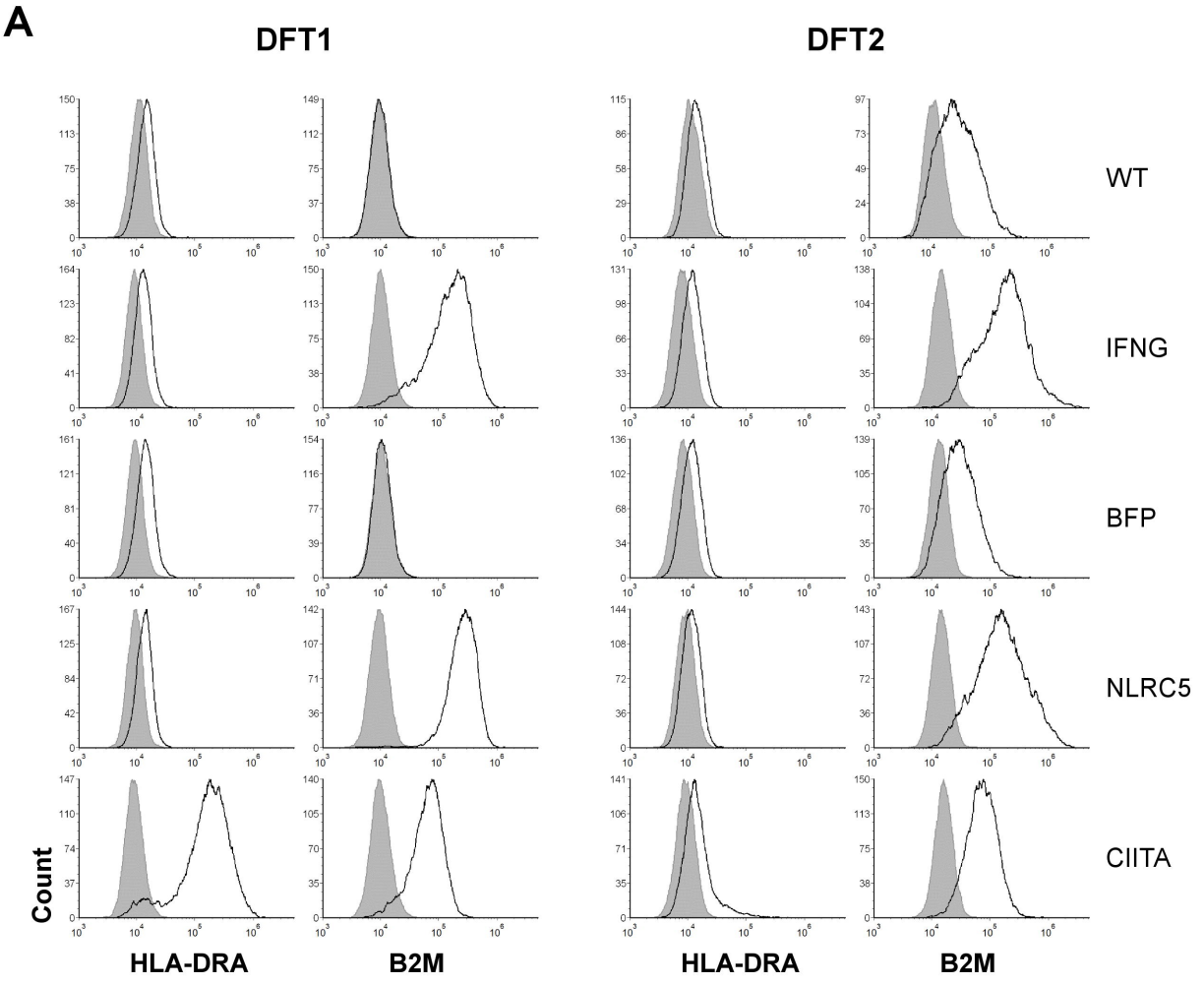
A
DFT1
DFT2
WT
IFNG
BFP
NLRC5
CIITA
Count
HLA-DRA
B2M
HLA-DRA
B2M

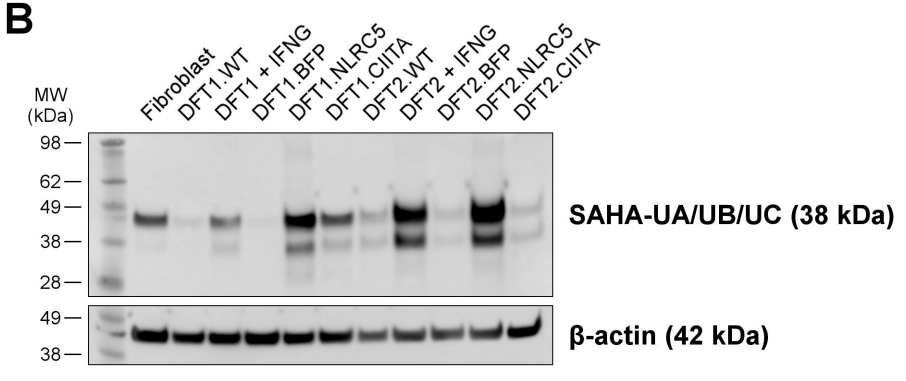
B
MW (kDa)
Fibroblast
DFT1.WT
DFT1 + IFNG
DFT1.BFP
DFT1.NLRC5
DFT1.CIITA
DFT2.WT
DFT2 + IFNG
DFT2.BFP
DFT2.NLRC5
DFT2.CIITA
98
62
49
38
28
SAHA-UA/UB/UC (38 kDa)
49
38
β-actin (42 kDa)

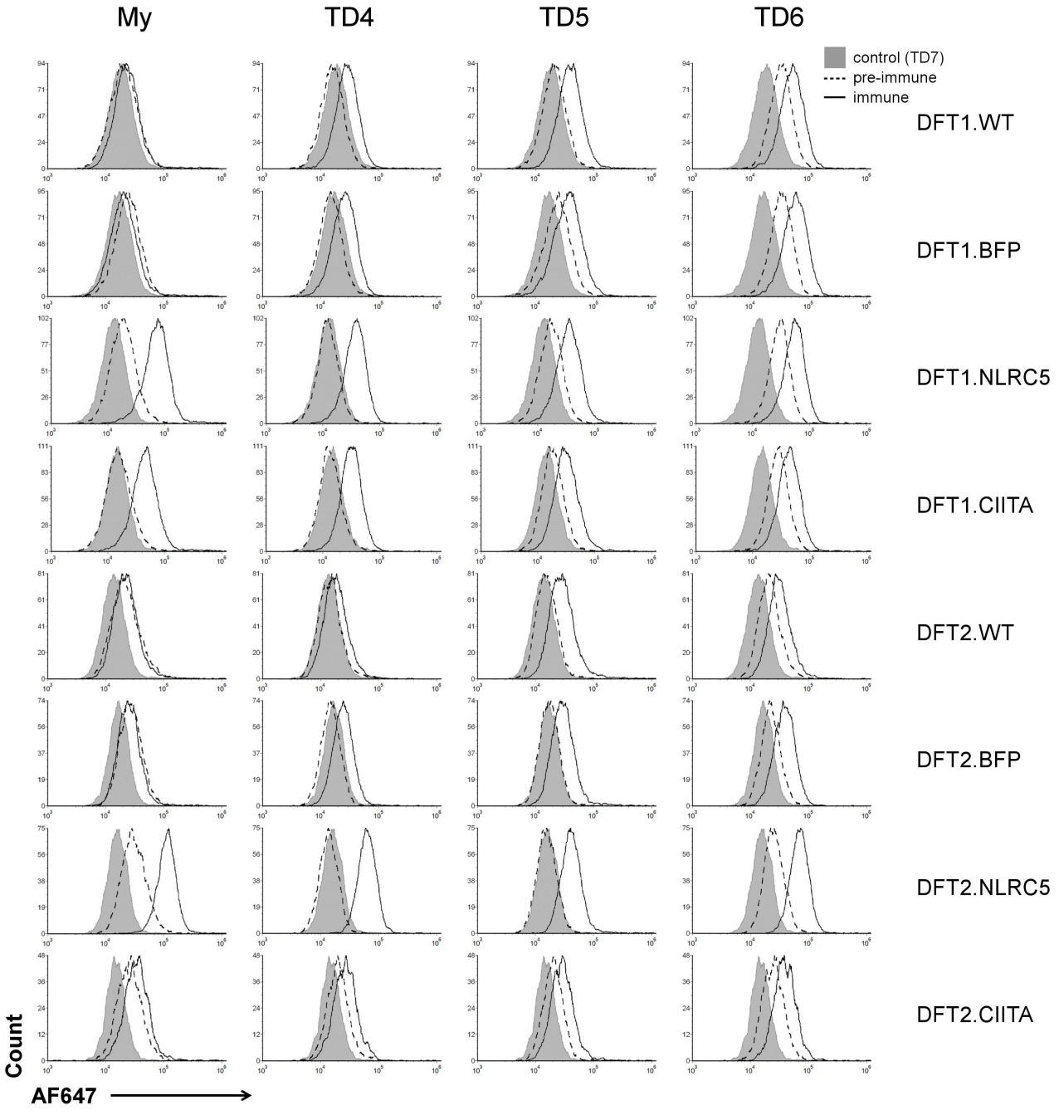
My
TD4
TD5
TD6
control (TD7)
pre-immune
immune
DFT1.WT
DFT1.BFP
DFT1.NLRC5
DFT1.CIITA
DFT2.WT
DFT2.BFP
DFT2.NLRC5
DFT2.CIITA
Count
AF647